ORIGINAL PAPER

CrossMark

Magnesium ion-conducting gel polymer electrolytes based on poly(vinylidene chloride-co-acrylonitrile) (PVdC-co-AN): a comparative study between magnesium trifluoromethanesulfonate (MgTf$_2$) and magnesium bis(trifluoromethanesulfonimide) (Mg(TFSI)$_2$)

D. Hambali [1,2] · N. H. Zainol [1,2] · L. Othman [1,2] · K. B. Md Isa [1,3] · Z. Osman [1,2]

Abstract

In this paper, we report the effects of two different type of salts which are magnesium trifluoromethanesulfonate (MgTf$_2$) and magnesium bis(trifluoromethanesulfonimide) (Mg(TFSI)$_2$) on ionic conductivity studies, transference number measurements, and electrochemical properties of gel polymer electrolyte (GPE) systems. Both systems used poly(vinylidene chloride-co-acrylonitrile) (PVdC-co-AN) as the host polymer with the incorporation of plastic crystal succinonitrile (SN) and plasticizer ethylene carbonate (EC) in the ratio of (1:1). The system containing Mg(TFSI)$_2$ exhibits higher in ionic conductivity of $\sim (10^{-7}$–$10^{-6})$ S cm^{-1} compared to the system containing MgTf$_2$ of $\sim (10^{-8}$–$10^{-7})$ S cm^{-1}. The conductivity temperature dependence studies of both GPE systems seem to obey the VTF relation. The ionic transference numbers were found to be > 0.9 for all GPEs while the highest cationic transference numbers obtained were 0.56 and 0.59 for MgTf$_2$ system and Mg(TFSI)$_2$ system, respectively. In linear sweep voltammetry (LSV) studies, wider electrochemical stability window was observed for the GPE containing Mg(TFSI)$_2$ than that containing MgTf$_2$ while cyclic voltammetry (CV) confirmed the conduction of Mg^{2+} ions in the GPEs. The structural and complex formations of the GPEs were confirmed by X-ray diffraction (XRD) analysis and both systems are shown to be amorphous in nature. The Mg/GPE/MgMn$_2$O$_4$ cells were assembled by using the most optimum GPE film from both systems and their charge-discharge performance was studied.

Keywords Gel polymer electrolytes · PVdC-co-AN · Conductivity · Transference number · Magnesium salts

Introduction

In these recent years, high performance and environmentally friendly rechargeable batteries have been a major global interest due to their considerable attentions while lithium-ion-based batteries have been the best candidate in view of its specific capacity and cycle stability [1, 2]. However, due to some drawbacks of lithium which are relatively expensive and suffer some safety issues, magnesium ion-based batteries have been introduced to replace lithium because of its performance capabilities closed to lithium [2, 3]. The abundance of magnesium in the earth's crust, low in atomic weight, low cost, environmentally benign (green), and electrochemically active (equivalent weight 12.15/Faraday) in nature and also can serve as a potential negative electrode (electrochemical potential −2.37 V vs. standard hydrogen electrode) [4–6] are also some of the advantages of magnesium to be a prospective replacement over lithium.

Basically, a battery consists of one or more electrochemical cells connecting together in series or parallel and the term "cell" composed of three major components which are the anode (negative electrode), cathode (positive electrode), and the electrolyte (ionic conductor). In this research work, the study is focusing on the electrolyte on the account that the

✉ Z. Osman
zurinaosman@um.edu.my

1   Centre for Ionics University of Malaya, University of Malaya, 50603 Kuala Lumpur, Malaysia

2   Department of Physics, University of Malaya, 50603 Kuala Lumpur, Malaysia

3   National Nanotechnology Centre, Ministry of Science, Technology and Innovation, 62620 Putrajaya, Malaysia

conventional liquid electrolyte has many disadvantages such as leakage problems, internal shorting, and highly reactive nature toward the electrode surfaces [7], although they possesses high in ionic conductivity. Gel polymer electrolytes (GPEs) currently have received high consideration as they can offer systems that are safer because they are less reactive, can reduce leakage, lighter, and more flexible in shape compared with liquid electrolytes [2, 8, 9]. It is made by the impregnation of large amount of liquid electrolytes into the polymer matrix [10, 11], and there are various research works that have been made on preparing gel polymer electrolytes with magnesium salts incorporated into it. Some examples are the systems of PEO/PMA-EC-DMC-Mg[(CF$_3$SO$_2$)2 N]$_2$ [12], P(VdF-*co*-HFP)-EC/PC-SiO$_2$-Mg(ClO$_4$)$_2$ [4], chitosan-Mg(Tf)$_2$-EMITfn [13], and PVA/PAN-Mg(ClO$_4$)$_2$ [14]. In addition, a new plastic crystal material which is succinonitrile (SN) has been introduced into the polymer electrolytes. It exhibits properties of high dielectric constant (~ 55), low melting temperature (54 °C), and plasticizing property [15] which can greatly help in dissolving salts as well as produce polymer electrolytes film that is good in mechanical stability. For example, the research done on P(VdF-HFP)-SN complexed with four different types of lithium salts and the addition of SN greatly enhances ionic conductivities of the polymer electrolytes due to the high polarity and diffusivity of SN [11]. Other than that, research done by Taib et al. [16] has proved that the use of SN can improve the electrochemical properties of chitosan-SN-LiTFSI-based SPEs. They obtained higher value of lithium ion transport number of 0.598 compared to the sample without SN, i.e., 0.119. The sample with SN also showed high electrochemical stability of 4.7 V.

However, to the best of the authors' knowledge, research on SN have been done only on lithium-based electrolytes and the addition of SN into the magnesium-based electrolyte has been pioneered in this research work by using two types of magnesium salts which are magnesium trifluoromethanesulfonate (MgTf$_2$) and magnesium bis(trifluoromethanesulfonimide) (Mg(TFSI)$_2$) and a comparative study between these two types of salt was done. Gel polymer electrolytes (GPEs) have been prepared by using poly(vinylidene chloride-co-acrylonitrile) (PVdC-co-AN) as the host polymer with the combination of SN with plasticizer ethylene carbonate (EC) in the ratio of (1:1) to make them as double plasticized GPEs. The use of double plasticizers is mainly because of the argument by Pistoia et al. [17] who discovered the advantages of binary plasticizers and the good combination of plasticizers will not only improve the ion dissociation but will also balance their unique characteristics and at the same time improve the interfacial properties. The ionic conductivity studies, transference number measurements, and electrochemical and structural studies were also carried out, and the optimum GPE samples from both magnesium

salt-system were used as electrolyte in magnesium ion cell. The charge-discharge profile of the cells has been analyzed.

Reagents and materials

Polyvinylidene (chloride-co-acrylonitrile) (PVdc-co-AN), (M$_w$ ~ 150,000 g/mol), succinonitrile (SN), magnesium trifluoromethanesulfonate (MgTf$_2$), and magnesium bis(trifluoromethanesulfonimide) (Mg(TFSI)$_2$) were obtained from Sigma-Aldrich while ethylene carbonate (EC) was obtained from Merck. All reagents were used as received without further modification.

Preparation of gel polymer electrolytes

The gel polymer electrolytes were prepared by using solution casting technique as in our previous reported paper [18]. In this work, EC plasticizer was added to the single plasticized GPE with the ratio of 1:1 (SN:EC) to become double plasticized GPE system while MgTf$_2$ and Mg(TFSI)$_2$ salts were varied from 5 to 30 wt%. All the GPE samples were kept in the desiccator for further investigations.

Characterization techniques

The glass transition temperatures, T_g, of the GPEs were determined by differential scanning calorimetry (DSC) using Pelkin Elmer DSC instrument in the temperature range of − 100 to 150 °C at heating rate of 10 °C/min under nitrogen atmosphere.

The room temperature ionic conductivity of GPE films were determined by AC impedance method using a HIOKI 3533 LCR bridge over the frequency range of 10 Hz to 200 kHz. The GPE film was placed between the stainless steel electrodes of the cell holder to perform the impedance measurements and the Cole-Cole plot obtained was used to calculate the conductivity value from the bulk electrolyte resistance, R_b, according to the following equation:

$$\sigma = \frac{t}{R_b A} \tag{1}$$

where t is the thickness of the GPE film (cm) and A is the effective contact area between the electrode and the film; hence, the value of conductivity (σ) was calculated. The conductivity temperature dependence studies were also carried out for the GPE films by varying the temperature from 303 to 353 K.

Ionic transference number was determined by direct current (DC) polarization method proposed by Evans et al. [19]. In this method, a constant voltage of 0.1 V was applied across the highest conducting film from each system that is sandwiched between the two stainless steel (SS) electrodes SS/GPE/SS which act as blocking electrodes and the resulting current is measured as a function of time. The value of ionic transport number, t_i, was calculated by using Eq. (2);

$$t_i = i_T - \frac{i_e}{i_T} \qquad (2)$$

where i_e is electronic current and i_T is the total current. Cationic transference number is then determined after the confirmation of charge species in the polymer electrolyte system.

X-ray diffraction (XRD) was carried out to study the structural and crystallinity of the GPE films by using X'Pert PRO PANalytical diffractometer of Cu Kα radiation ($\lambda = 1.5406$ Å).

Linear sweep voltammetry (LSV) was performed to investigate the electrochemical stability of the GPEs by using a three-electrode cell with stainless steel as working electrode while magnesium as reference and counter electrodes with the cell configuration of SS/GPE/Mg. All LSV experiments were carried out at a sweep rate of 5 mV s^{-1} in the voltage range of 0–5 V (vs. Mg^{2+}/Mg) at room temperature. Cyclic voltammetry (CV) measurements of Mg/GPE/Mg cells were also performed at room temperature with a scan rate of 5 mV s^{-1} from − 5.0 to 5.0 V.

Cell performance

Magnesium ion cell was fabricated by using the most optimum GPE films from both MgTf$_2$ and Mg(TFSI)$_2$ systems. In this experiment, magnesium foil was used as a negative electrode while magnesium manganese oxide (MgMn$_2$O$_4$) as the positive electrode and the performance of the cell will be analyzed.

Results and discussion

Differential scanning calorimeter

The values of T_g for all samples are tabulated as in Table 1. Since T_g has the influence on the stiffness and flexibility of the polymer which in turn decides the value of T_g, the lower value of T_g indicates polymer with high flexibility while high value of T_g increase the stiffness of the polymer. In this case, GPE samples with 30 wt% of MgTf$_2$ and 15 wt% Mg(TFSI)$_2$ has the lowest T_g of 42 and 44 °C in each system, respectively. However, higher T_g values were observed in Mg(TFSI)$_2$ system compared to MgTf$_2$. These higher T_g can be explained by a greater degree of dissociation of TFSI salt because of their lower lattice energies

Table 1 The compositions and conductivity values of the GPE samples

Sample	Composition in weight ratio					Conductivity, σ (S cm^{-1})	Glass transition temperature, T_g, (°C)
	PVdC-co-AN	SN	EC	MgTf$_2$	Mg(TFSI)$_2$		
Pure PVdC-co-AN	100	0	0	0	0	7.35×10^{-10}	51
PVdC-co-AN-SN	70	30	0	0	0	1.82×10^{-9}	50
PVdC-co-AN-SN-EC	56	22	22	0	0	1.54×10^{-8}	50
GPE1	53	21	21	5	0	2.82×10^{-8}	47
GPE2	50	20	20	10	0	6.54×10^{-8}	46
GPE3	47	19	19	15	0	1.14×10^{-7}	44
GPE4	44	18	18	20	0	2.13×10^{-7}	43
GPE5	41	17	17	25	0	2.48×10^{-7}	43
GPE6	38	16	16	30	0	2.82×10^{-7}	42
GPE7	53	21	21	0	5	8.69×10^{-7}	48
GPE8	50	20	20	0	10	1.54×10^{-6}	47
GPE9	47	19	19	0	15	1.93×10^{-6}	44
GPE10	44	18	18	0	20	3.01×10^{-7}	47
GPE11	41	17	17	0	25	2.12×10^{-7}	49
GPE12	38	16	16	0	30	1.00×10^{-7}	49

Fig. 1 Complex impedance plots of **a** MgTf$_2$ system, **b** Mg(TFSI)$_2$ system, and **c** equivalent circuit in accordance of the impedance plots
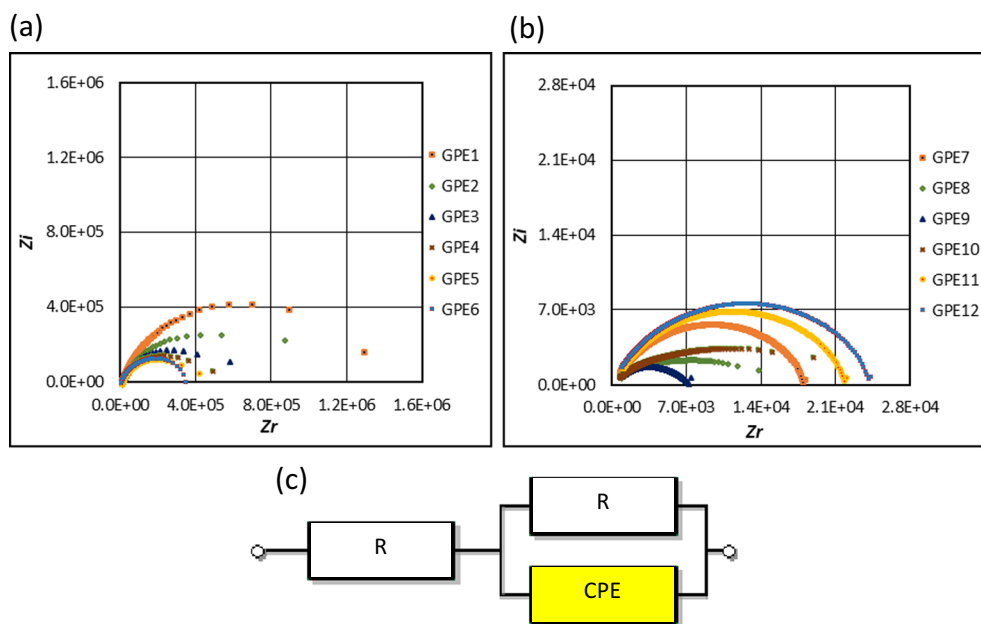
Ionic conductivity studies

Figure 1a, b represents the complex impedance plots of all the GPE samples for both MgTf$_2$ and Mg(TFSI)$_2$ systems. The impedance plot comprises of a distorted semicircular arc for all samples and the depressed semicircle can be explained by incorporating a constant phase element (CPE) in equivalent circuit as shown in Fig. 1c. This CPE replacing the capacitors in the circuit is a leaky capacitor, which has an intermediate characteristic between a resistor and a capacitor [21]. The analysis and fitting of the impedance data according to the equivalent circuit was performed by a ZIVE ZMAN 2.3 EIS

analysis software. The equivalent circuit is best described by a circuit composed of a resistor in parallel with a CPE that is connected in series with a resistor. The CPE is another generic distributed circuit element, arises from the fact that the electrode surface is normally rough and/or the bulk properties of the electrode material are inhomogeneous [22, 23]. The intercept of the semicircle with the real axis (Zr) in the low frequencies region is the bulk resistance (R_b). It can be observed that the values of R_b from Mg(TFSI)$_2$ system are lower than MgTf$_2$ system for all samples.

The ionic conductivities of all the GPE samples for both MgTf$_2$ and Mg(TFSI)$_2$ systems were then calculated by using Eq. (1) and tabulated as in Table 1. It can be seen from the table that the highest conductivity obtained are 2.82×10^{-7} S cm^{-1} and 1.93×10^{-6} S cm^{-1} for GPE samples

Fig. 2 Ionic conductivity of GPE samples with 5 to 30 wt% of **a** MgTf$_2$ salt and **b** Mg(TFSI)$_2$ salt
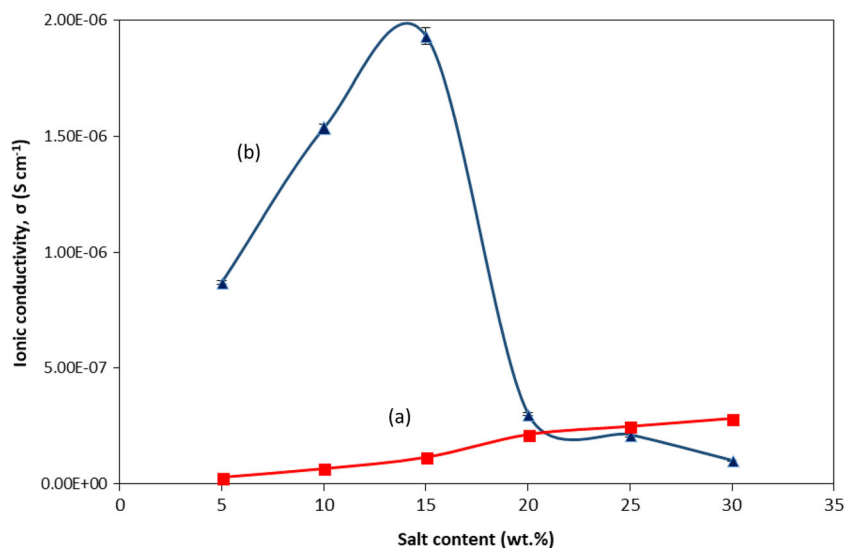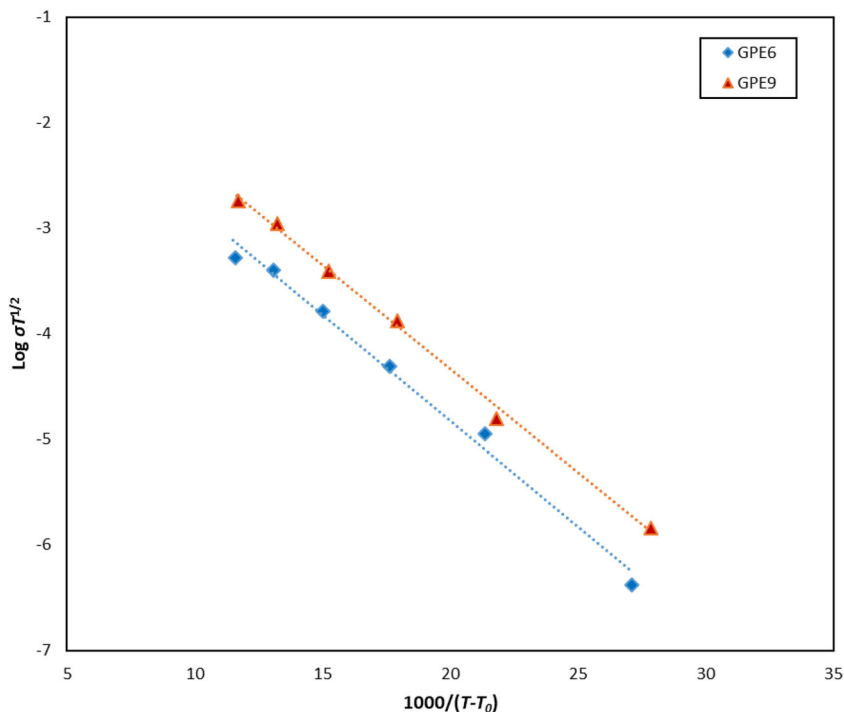
Fig. 4 Plot of log $\sigma T^{1/2}$ against $1000/(T-T_0)$ for GPE samples containing 30 wt% of $MgTf_2$ and 15 wt% of $Mg(TFSI)_2$

containing 30 wt% $MgTf_2$ and 15 wt% $Mg(TFSI)_2$, respectively. The conductivity is higher for sample containing $Mg(TFSI)_2$ salt because of the characteristics of the $-(TFSI)_2$ group. This type of anion was reported to have a highly delocalized anionic charge and a flexible structure and a larger ionic radius may result in the easier ionic dissociation of $Mg(TFSI)_2$ with the nitrile group of the polymer [18] compared with $MgTf_2$ salt [24, 25]. For better understanding on

the conductivity behavior, Fig. 2 was plotted to show the variation of conductivity for both systems with their respective weight percentage of magnesium salt. It is shown that the patterns of conductivity are not the same for both systems. For $MgTf_2$ system, the conductivity continually increases from 5 to 30 wt% of $MgTf_2$ salt attributed to the increase of the number of charge carrier, n, and ionic mobility, μ, as stated by the relation of $\sigma = nq\mu$, where q is the charge of mobile

Fig. 3 Plot of log σ against $1000/T$ for GPE samples containing 30 wt% of $MgTf_2$ and 15 wt% of $(MgTFSI)_2$
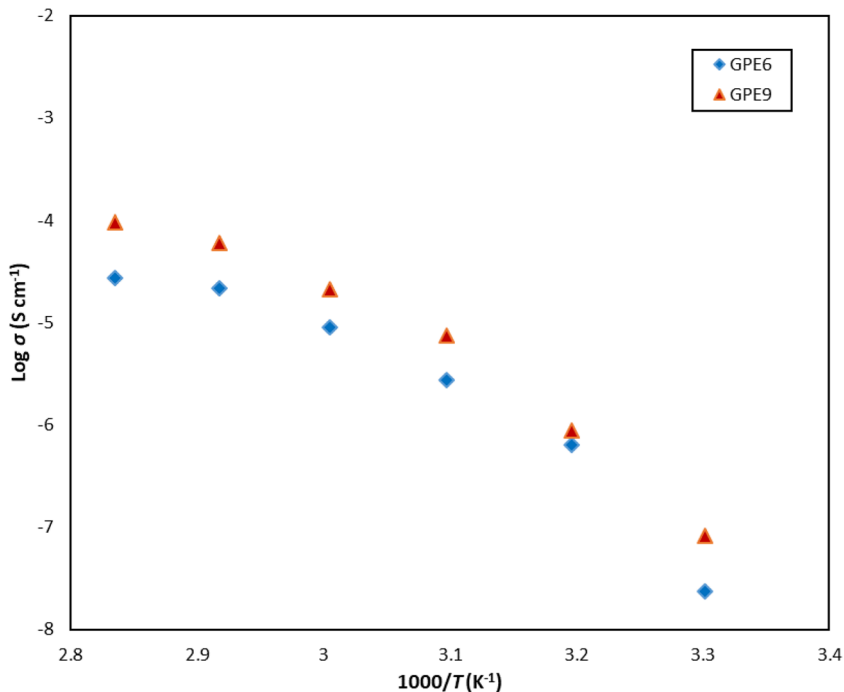
Table 2 The parameters of A_0, E_a, and T_0 by fitting of conductivity to VTF equation for 30 wt% of MgTf$_2$ and 15 wt% of Mg(TFSI)$_2$

Sample	A_0 (S cm^{-1} K$^{1/2}$)	E_a (eV)	T_0 (K)
GPE6	0.156	0.040	265
GPE9	0.399	0.039	267

carrier. The enhancement of conductivity with salt also suggest that there is an increase in concentration of free Mg^{2+} ions in the polymer electrolyte matrix (not forming ion pair with bulkier anions) [26]. Nevertheless, further increasing on the concentration of MgTf$_2$ salt formed a GPE sample with precipitate which shows that the mixture is already saturated and thus, 30 wt% of MgTf$_2$ salt is the maximum concentration.

On the other hand, for Mg(TFSI)$_2$ system, the conductivity increased from 5 to 15 wt% of Mg(TFSI)$_2$ salt due to the same arguments but decreased considerably when 20 wt% of salt was added and continually to decrease until the maximum 30 wt% of salt added with the lowest conductivity of $1.00 \times$

10^{-7} S cm^{-1}. This observation suggests that the ionic conductivity is not a simple linear function of concentration as there is a concentration window for optimizing the conductivity [27]. The reduce in conductivity is related to a greater cation-anion interactions competing for coordination of magnesium cations on the PVdC-co-AN nitrile group and also the drastic increase in viscosity (or lower mobility) of the mixture [28].

Temperature dependence ionic conductivity

The relationship between ionic conductivity with temperature was also evaluated by operating temperature dependence ionic conductivity studies for the GPEs at a temperature range of 303 to 353 K. Figure 3 depicts the plot of log σ against 1000/T for the selected GPE samples containing 30 wt% MgTf$_2$ and 15 wt% Mg(TFSI)$_2$, i.e., the highest conducting sample from both systems. The variation of log σ with reciprocal temperature shows a non-linear behavior for each film and suggesting that the ionic conduction in GPE system does not obey Arrhenius rule. In this case, the molecular motion involves
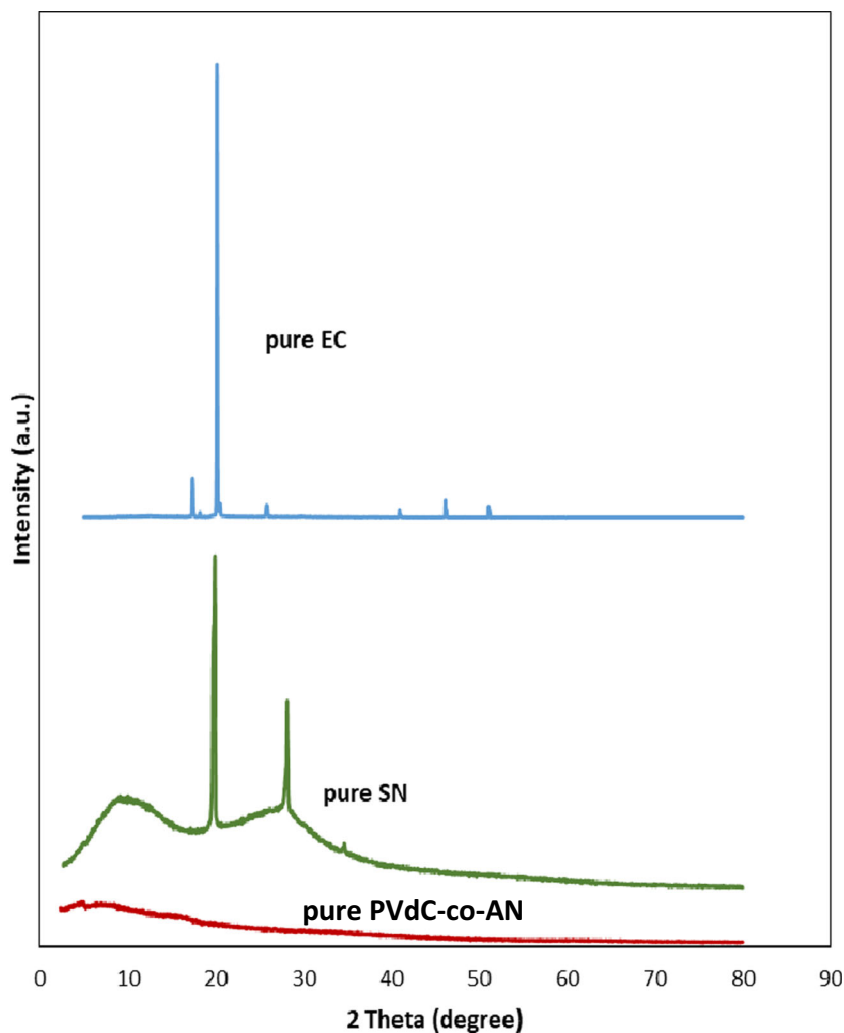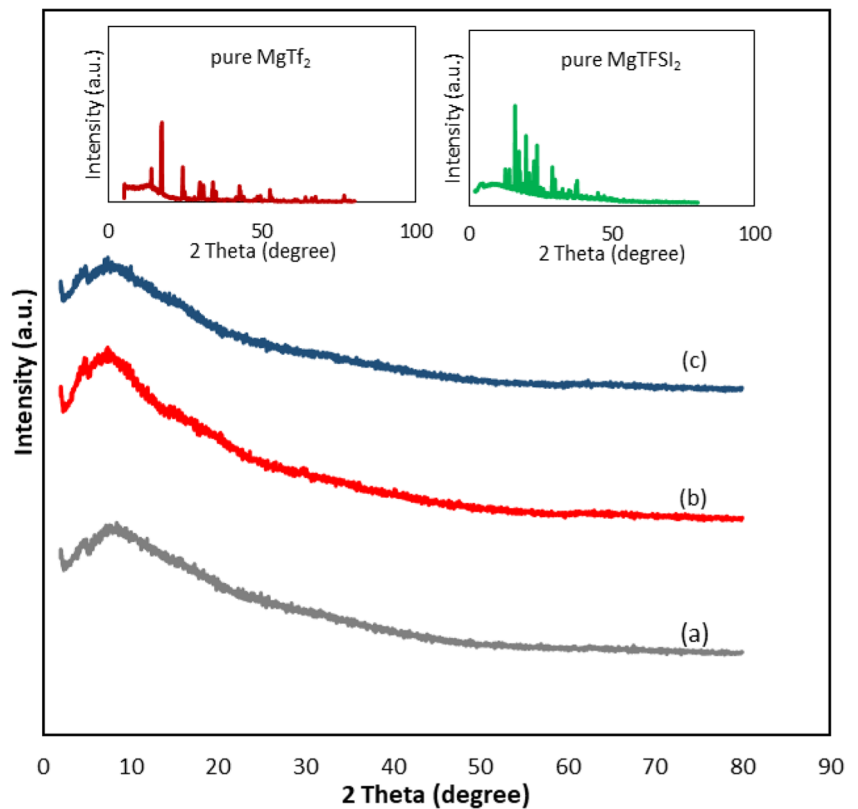

Fig. 5 X-ray diffractograms of pure PVdC-co-AN, pure SN, and pure EC

Fig. 6 X-ray diffractograms of (**a**) PVdC-co-AN-SN-EC, (**b**) PVdC-co-AN-SN-EC-30 wt% MgTf$_2$, and (**c**) PVdC-co-AN-SN-EC-15 wt% Mg(TFSI)$_2$. Inset graphs show X-ray diffractograms of pure MgTf$_2$ and Mg(TFSI)$_2$

the availability of vacancies and the polymer chain, where ions or solvated molecules can move freely into it. This leads to the increase in conductivity due to the increase in the overall mobility of ions and polymer that will assist ion transport and consequently compensate the retarding effect of ion clouds [29, 30]. In other words, the ion transport in polymer electrolytes is dependent on polymer segmental motion and moves through the plasticizer-rich phase where the characteristic of

the viscous matrix involves plasticizer, salt, and polymer themselves [18, 20, 29, 31] as described by a Vogel-Tamman-Fulcher (VTF) behavior [32] in Eq. (3):

$$\sigma(T) = A_0 T^{-1/2} \, exp(-E_a/(T-T_0)) \tag{3}$$

where the constants A_0 is the pre-exponential factors related to the number of charge carriers, and E_a is a pseudo-activation energy associated with the rate at which viscosity changes with temperature [2] and T_0 is close to the glass transition temperature, T_g. In this work, we considered $T_0 = T_g - 50$ K. Before further analysis, it is cleared that VTF model has some restrictions in application. This model can be applied to amorphous electrolytes with completely dissociated salts as verified by XRD analysis which will be discussed further. It can also be applied rather to compare properties of family of samples with similar structure [33]. The VTF empirical relation can be observed by a linear variation between log $\sigma T^{1/2}$ against $1000/(T-T_0)$ for the highest conducting sample from both systems as shown in Fig. 4 and the parameters A_0, E_a, and T_0 is as shown in Table 2. The E_a values for both GPE samples is very low which is 0.040 and 0.039 for sample containing 30 wt% MgTf$_2$ and 15 wt% Mg(TFSI)$_2$, respectively, thus indicates a relatively easy ion migration in the electrolyte system [34]. For A_0 values, the value is greater for Mg(TFSI)$_2$ system compared to MgTf$_2$ system

Table 3 The values of ionic transference numbers of GPE samples

Sample	Ionic transference number, t_i
GPE1	0.93
GPE2	0.95
GPE3	0.96
GPE4	0.96
GPE5	0.97
GPE6	0.99
GPE7	0.96
GPE8	0.98
GPE9	0.99
GPE10	0.95
GPE11	0.95
GPE12	0.94

Fig. 7 DC polarization plots for GPE samples containing **a** 30 wt% of MgTf$_2$ and **b** 15 wt% of Mg(TFSI)$_2$. Inset graph shows the impedance plots (i) before and (ii) after DC polarization
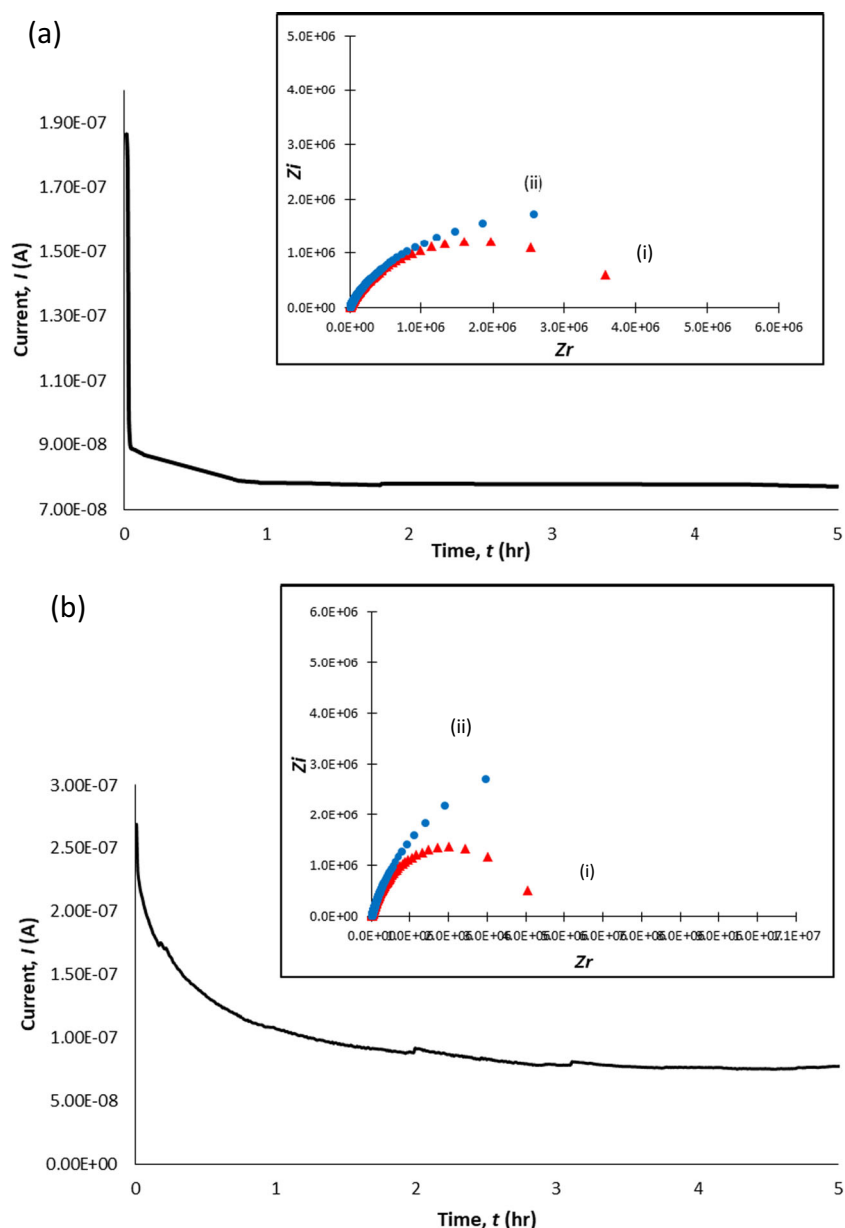
in accordance with the value of room temperature conductivity, i.e., the conductivity value for Mg(TFSI)$_2$ system is higher than that of MgTf$_2$ system despite only a small difference in value. This is because of the argument by Kumar et al. [30], a large variation of A_0 could not be explained, although the variation of A_0 could be attributed to the difference in ionic concentrations, due to a small variation of ionic concentration on account of other terms such as the jump distance, vibrational frequency, etc., which might influence A_0. These terms were unlikely to vary very much in the polymer electrolyte system, and the large variation in magnitude of A_0 was explained as being due to an entropy term.

Structural properties

Figure 5 shows X-ray diffractograms of pure PVdC-co-AN, pure SN, and pure EC. The pure PVdC-co-AN shows only a broad peak at $2\theta = 7.5°$ indicates that it is amorphous in nature while for pure SN and EC, there exist several sharp peaks which show that they are crystalline in nature. After the complexation of polymer with SN and EC, all peaks associate with them disappeared as shown in Fig. 6. This suggests that the PVdC-co-AN-SN-EC sample has become completely amorphous and the role of SN and EC as plasticizer can be seen here. The absence of peaks of SN, EC, and MgTf$_2$ and Mg(TFSI)$_2$ salts after the incorporation of salts in the XRD

Fig. 8 Linear sweep voltammogram for the GPE sample containing 30 wt% MgTf$_2$. Inset graph shows linear sweep voltammogram for the GPE sample containing 15 wt% Mg(TFSI)$_2$
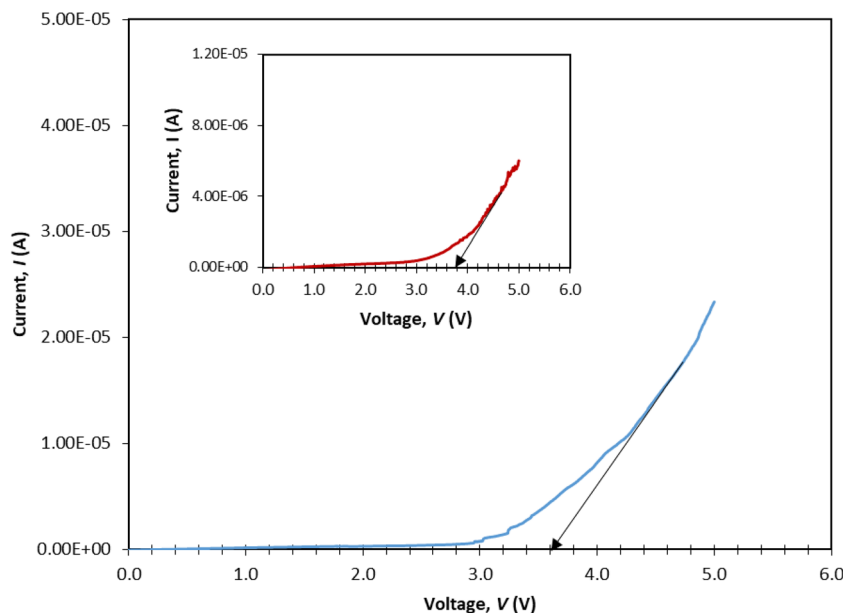
patterns also revealed a perfect salt complexation with the polymer matrix [35, 36].

Transference number

The values of ionic transference numbers, ti are calculated using Eq. (2) and the values are found to be greater than 0.9 for all GPE samples as shown in Table 3. This shows that the charge carriers in the GPEs are predominantly due to ions and the samples are ionic conductors. The results agreed with the argument that no electronic conductivity is expected in the gel-like electrolytes where liquid electrolytes are entrapped in the almost inert network of polymer hosts and liquid-like charge transport takes place in such systems [37]. Likewise, there are different ionic species expected to be mobile in the gel polymer electrolytes system which are Mg^{2+} and Tf$^-$ ions for MgTf$_2$ samples and Mg^{2+} and TFSI$^-$ ions for MgTFSI$_2$ samples. Therefore, a method has been proposed by Evans et

al. [19] using the combination of AC impedance and DC polarization techniques to evaluate the transference number Mg^{2+} ions in the polymer electrolytes. In this technique, magnesium foil was used with cell configuration of Mg/GPE/Mg and the cell has been polarized by applying a constant voltage of 0.1 V for about 5 h and the value of initial and final currents, I_0 and I_s, were recorded. AC impedance was measured before and after polarization to obtain the values of electrode-electrolyte resistances. Thus, the magnesium ions transference number, t_{Mg2+}, can be determined by using Eq. (4);

$$t_{Mg2+} = \frac{I_s}{I_0}\left[\frac{\Delta V - I_0 R_0}{\Delta V - I_s R_s}\right] \tag{4}$$

where I_0 is the initial current and I_s is the final current, while R_0 and R_s are the cell resistance before and after polarization, respectively. The plot of DC polarization for the highest conducting film for both GPE systems is as shown in Fig. 7. From the figure, there is an initial current, I_0 at the very

Fig. 9 Cyclic voltammograms of Mg/GPE/Mg with highest conducting GPE of **a** MgTF$_2$ system and **b** Mg(TFSI)$_2$ system
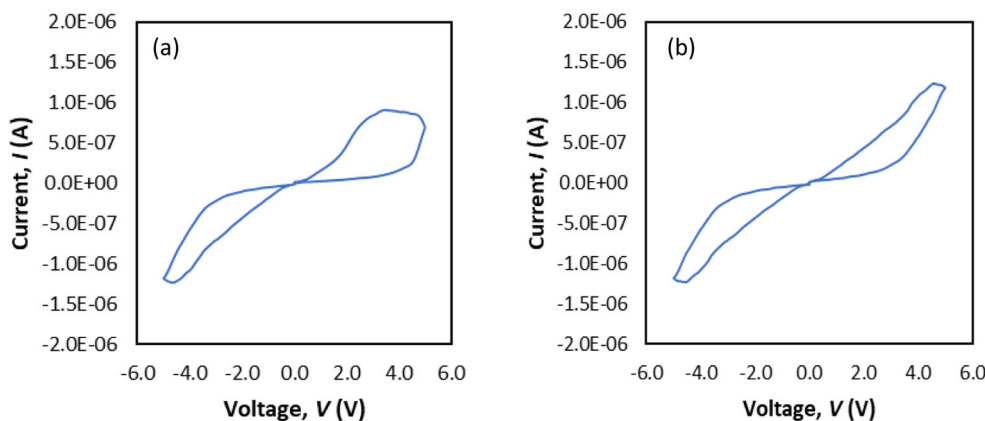
beginning and the current is then drop continuously due to the growth of passivation layers on the magnesium electrodes and this establishes the concentration gradient. After the polarization process, a steady-state current, I_s, is established and the inset graph of Fig. 7 shows the impedance plots from AC measurements before and after polarization to determine the values of cell resistances. The magnesium ion transference number, t_{Mg2+}, was then calculated using Eq. (4) and the values obtained are 0.56 and 0.59 for GPE containing 30 wt% $MgTf_2$ and 15 wt% $Mg(TFSI)_2$, respectively. This shows that the t_{Mg2+} of the GPE film containing $Mg(TFSI)_2$ is higher than that containing $MgTf_2$. However, both t_{Mg2+} values denoting a value > 0.5 and thus suggest substantial contributions of Mg^{2+} ions to the total conduction in the electrolyte system. The high value of t_{Mg2+} also can eliminate the concentration gradients within the battery so that the battery can operate under a high current density [38].

Linear sweep voltammetry

The electrochemical stability of the GPEs was investigated by linear sweep voltammetry to measure the breakdown voltage for the electrolyte so that it can withstand the operating voltage in the battery system. The measurements were carried out using SS/GPE/Mg cell (vs. Mg/Mg^{2+}) and Fig. 8 shows the voltammogram for the sample containing 30 wt% $MgTf_2$ and the inset graph for the sample containing 15 wt% $Mg(TFSI)_2$. From both plots, it can be observed that there is a very low background current measured in a potential region between 0 and 3.6 V for 30 wt% $MgTf_2$ sample and 3.8 V for 15 wt% $Mg(TFSI)_2$ sample. The small current might be attributed to the change of the

stainless steel surface [39]. The current then began to flow and increased rapidly upon reaching the cut-off voltage which indicates that the electrolyte decomposition process has taken place [7, 10]. The cut-off voltage, i.e., the onset decomposition voltage is higher for GPE sample containing $Mg(TFSI)_2$ compared with that containing $MgTf_2$. This shows that sample containing $Mg(TFSI)_2$ is more electrochemically stable as the capability of the polymer electrolyte to withstand high voltages at the cathode interface [40] is higher than sample containing $MgTf_2$. As rechargeable batteries generally operate between 3.0 and 4.5 V, it can be concluded that both films are suitable to be used as an electrolyte in rechargeable magnesium battery.

Cyclic voltammetry

Cyclic voltammograms of the highest conducting sample for both systems are shown in Fig. 9. A pair of cathodic and anodic features is observed on the magnesium working electrode of each sample. The deposition of magnesium begins at relatively low overpotential vs. Mg/Mg^{2+}. The nature of oxidation and reduction peaks indicate the reversible Mg^{2+} intercalation/deintercalation processes and suggests that the cathodic deposition and anodic oxidation of magnesium are facile at the Mg/GPE. This result confirmed the existence of Mg^{2+} ion conduction in the GPEs [38, 41, 42].

Mg/GPE/MgMn$_2$O$_4$ cell analysis

Figure 10 shows the discharge capacity as a function of cycle number for the highest conducting GPE of both systems. It can be observed that the discharge capacity

Fig. 10 The discharge capacity with cycle for the GPE sample containing 30 wt% $MgTf_2$. Inset graph shows the discharge capacity with cycle for the GPE sample containing 15 wt% $Mg(TFSI)_2$
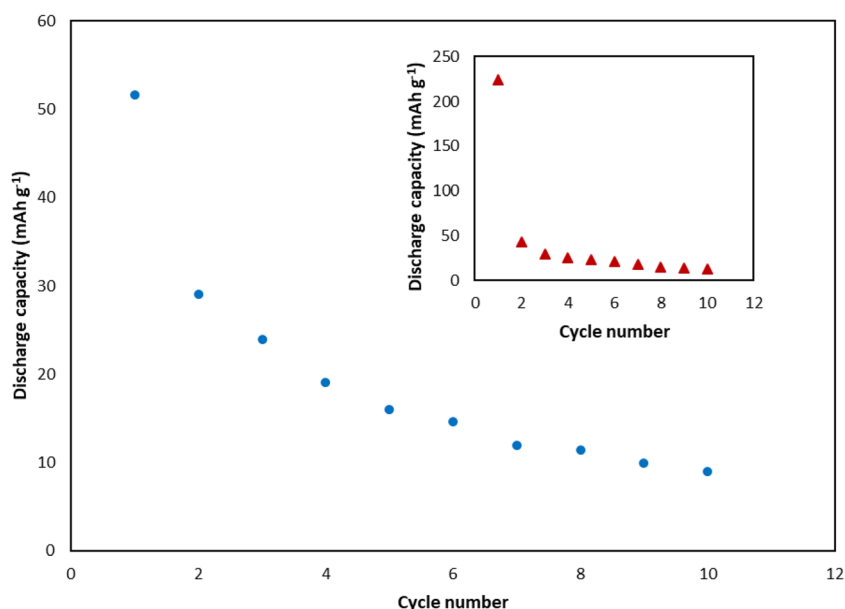
decreased rapidly between the first and second cycle and continued to decline with subsequent cycling with the initial capacity of 51 and 223 mAh g^{-1} for $MgTF_2$ and $Mg(TFSI)_2$ system, respectively. The decline of discharge capacity with cycling is attributed to the formation of Mg/GPE interface layer, where the passivation film grows in thickness during the repeating cycling [4, 43]. As a consequent, the internal resistance increased and will block the charge transfer between the Mg anode and GPE resulting in the loss of discharge capacity during cycling. As the discharge capacity of GPE containing $Mg(TFSI)_2$ salt is higher than that of $MgTF_2$, it indicates that $Mg(TFSI)_2$ system has better performance as magnesium ion cell or rechargeable magnesium battery in practical level. However, further work is in progress to achieve higher cell capacity and improve cycling performance with these gel polymer electrolytes.

Conclusions

Double plasticized GPEs containing PVdC-co-AN, SN, and EC have been prepared with varied concentrations of $MgTf_2$ and $Mg(TFSI)_2$ salts from 5 to 30 wt% and a comparative study has been done between these two types of magnesium salt. The maximum room temperature ionic conductivity obtained is higher for GPE sample containing 15 wt% $Mg(TFSI)_2$ which is 1.93×10^{-6} S cm^{-1} while for $MgTf_2$ system, the value is 2.82×10^{-7} S cm^{-1}. The temperature dependence ionic conductivity studies of the GPEs have found to obey the VTF behavior. The ionic transport number values obtained are greater than 0.9 which shows the charge carriers in both GPE systems are predominantly ions. The magnesium ion transference number, t_{Mg2+}, obtained are 0.56 and 0.59 for GPE containing 30 wt% $MgTf_2$ and 15 wt% $Mg(TFSI)_2$, respectively, and suggest that Mg^{2+} ions give substantial contributions to the total conductivity in the electrolyte system. The amorphousity of the GPE systems has been confirmed by XRD analysis. In LSV studies, the highest conducting $Mg(TFSI)_2$ is more electrochemically stable than that of containing $MgTf_2$ while CV confirmed the conduction of Mg^{2+} ions in the GPEs. The GPEs have been fabricated as magnesium ion cell and obtained discharge capacity for the first cycle of 51 and 223 mAh g^{-1} for $MgTF_2$ and $Mg(TFSI)_2$ system, respectively. As a whole, the GPEs in this study need to be improved and studied further to obtain better performance for magnesium rechargeable battery.

References

1. Tarascon J-M, Armand M (2001) Issues and challenges facing rechargeable lithium batteries. Nature 414:359–367

2. Pandey GP, Hashmi SA (2009) Experimental investigations of an ionic-liquid-based, magnesium ion conducting, polymer gel electrolyte. J Power Sources 187:627–634

3. Asmara SN, Kufian MZ, Majid SR, Arof AK (2011) Preparation and characterization of magnesium ion gel polymer electrolytes for application in electrical double layer capacitors. Electrochim Acta 57:91–97

4. Oh J, Ko J, Kim D (2004) Preparation and characterization of gel polymer electrolytes for solid state magnesium batteries. Electrochim Acta 50:903–906

5. Saha P, Kanchan M, Velikokhatnyi OI (2014) Progress in materials science rechargeable magnesium battery: current status and key challenges for the future. Prog Mater Sci 66:1–86

6. Kumar GG, Munichandraiah N (2000) Solid-state Mg/MnO$_2$ cell employing a gel polymer electrolyte of magnesium triflate. J Power Sources 91:157–160

7. Saikia D, Wu HY, Pan YC, Lin CP, Huang KP, Chen KN, Fey GTK, Kao HM (2011) Highly conductive and electrochemically stable plasticized blend polymer electrolytes based on PVdF-HFP and triblock copolymer PPG-PEG-PPG diamine for Li-ion batteries. J Power Sources 196:2826–2834

8. Raghavan P, Choi JW, Ahn JH, Cheruvally G, Chauhan GS, Ahn HJ, Nah C (2008) Novel electrospun poly(vinylidene fluoride-co-hexafluoropropylene)-in situ SiO$_2$ composite membrane-based polymer electrolyte for lithium batteries. J Power Sources 184:437–443

9. Raghavan P, Zhao X, Kim J et al (2008) Ionic conductivity and electrochemical properties of nanocomposite polymer electrolytes based on electrospun poly (vinylidene fluoride-co-hexafluoropropylene) with nano-sized ceramic fillers. Electrochim Acta 54:228–234

10. Yang C-M, Kim H-S, Na B-K, Kum KS, Cho BW (2006) Gel-type polymer electrolytes with different types of ceramic fillers and lithium salts for lithium-ion polymer batteries. J Power Sources 156:574–580

11. Fan L, Wang X, Long F (2009) All-solid-state polymer electrolyte with plastic crystal materials for rechargeable lithium-ion battery. J Power Sources 189:775–778

12. Yoshimoto N, Yakushiji S, Ishikawa M, Morita M (2003) Rechargeable magnesium batteries with polymeric gel electrolytes containing magnesium salts. Electrochim Acta 48:2317–2322

13. Wang J, Song S, Gao S, Muchakayala R, Liu R, Ma Q (2017) Mg-ion conducting gel polymer electrolyte membranes containing biodegradable chitosan: preparation, structural, electrical and electrochemical properties. Polym Test 62:278–286

14. Manjuladevi R, Thamilselvan M, Selvasekarapandian S, Mangalam R, Premalatha M, Monisha S (2017) Mg-ion conducting blend polymer electrolyte based on poly (vinyl alcohol) - poly (acrylonitrile) with magnesium perchlorate. Solid State Ionics 308:90–100

15. Alarco P-J, Abu-Lebdeh Y, Abouimrane A, Armand M (2004) The plastic-crystalline phase of succinonitrile as a universal matrix for solid-state ionic conductors. Nat Mater 3:476–481

16. Taib NU, Hayati N (2014) Plastic crystal–solid biopolymer electrolytes for rechargeable lithium batteries. J Memb Sci 468:149–154

17. Pistoia G, De Rossi M, Scrosati B (1970) Study of the behavior of ethylene carbonate as a nonaqueous battery solvent. J Electrochem Soc 117:500

18. Hambali D, Zainuddin Z, Osman Z (2016) Characteristics of novel plastic crystal gel polymer electrolytes based on PVdC-co-AN. Ionics 23:285–294

19. Evans J, Vincent CA, Bruce PG (1987) Electrochemical measurement of transference numbers in polymer electrolytes. Polymer 28: 2324–2328

20. Lee DK, Allcock HR (2010) The effects of cations and anions on the ionic conductivity of poly [bis (2-(2-methoxyethoxy) ethoxy) phosphazene] doped with lithium and magnesium salts of trifluoromethanesulfonate and bis (trifluoromethanesulfonyl) imidate. Solid State Ionics 181:1721–1726

21. Pradhan DK, Samantaray BK, Choudhary RNP et al (2007) Effect of plasticizer on structural and electrical properties of nanocomposite solid polymer electrolytes. Int J Electrochem Sci 2:861–871

22. Fernández-Sánchez C, McNeil CJ, Rawson K (2005) Electrochemical impedance spectroscopy studies of polymer degradation: application to biosensor development. TrAC Trends Anal Chem 24:37–48

23. Osman Z, Samin SM, Othman L, Md Isa KB (2012) Ionic transport in PMMA-NaCF$_3$SO$_3$ gel polymer electrolyte. Adv Mater Res 545: 259–263

24. Marzantowicz M, Dygas JR, Krok F, Tomaszewska A, Florjańczyk Z, Zygadło-Monikowska E, Lapienis G (2009) Star-branched poly(ethylene oxide) LiN(CF$_3$SO$_2$)$_2$: a promising polymer electrolyte. J Power Sources 194:51–57

25. He D, Kim DW, Park JS, Cho SY, Kang Y (2013) Electrochemical properties of semi-interpenetrating polymer network solid polymer electrolytes based on multi-armed oligo(ethyleneoxy) phosphate. J Power Sources 244:170–176

26. Jayaraman R, Vickraman P, Subramanian NMV, Justin AS (2016) A.C. impedance, XRD, DSC, FTIR studies on PbTiO$_3$ dispersoid pristine PVdF-co-HFP and PEMA blended PVdF-co-HFP microcomposite electrolytes. J Non-Cryst Solids 435:27–32

27. Echeverri M, Kim N, Kyu T (2012) Ionic conductivity in relation to ternary phase diagram of poly(ethylene oxide), succinonitrile, and lithium bis(trifluoromethane)sulfonimide blends. Macromolecules 45:6068–6077

28. Lascaud S, Perrier M, Vallee A, Besner S, Prud'homme J, Armand M (1994) Phase diagrams and conductivity behavior of poly(ethylene oxide)-molten salt rubbery electrolytes. Macromolecules 27: 7469–7477

29. Rajendran S, Mahendran O, Kannan R (2002) Ionic conductivity studies in composite solid polymer electrolytes based on methylmethacrylate. J Phys Chem Solids 63:303–307

30. Kumar GG, Munichandraiah N (2000) Effect of plasticizers on magnesium-poly (ethyleneoxide) polymer electrolyte. J Electron Chem 495:42–50

31. Pradeepa P, Edwin S, Sowmya G et al (2016) Optimization of hybrid polymer electrolytes with the effect of lithium salt concentration in PEO/PVdF-HFP blends. Mater Sci Eng B 205:6–17

32. Ratner MA, Shriver DF (1988) Ion transport in solvent-free polymers. Chem Rev 88:109–124

33. Piszcz M, Zhang H, Marczewski M, Żukowska GZ, Lemańska K, Sukiennik M, Siekierski M (2017) Vibrational spectroscopic studies combined with viscosity analysis and VTF calculation for hybrid polymer electrolytes. Solid State Ionics 303:78–88

34. Kumar R, Rhee H (2012) Effect of succinonitrile on electrical, structural, optical, and thermal properties of [poly(ethylene oxide)-succinonitrile]/LiI–I$_2$ redox-couple solid polymer electrolyte. Electrochim Acta 76:159–164

35. Zhou Y, Xiang W, Chen S, Fang S, Zhou X, Zhang J, Lin Y (2009) Influences of poly(ether urethane) introduction on poly(ethylene oxide) based polymer electrolyte for solvent-free dye-sensitized solar cells. Electrochim Acta 54:6645–6650

36. Kalaignan GP, Kang MS, Kang YS (2006) Effects of compositions on properties of PEO-KI-I$_2$ salts polymer electrolytes for DSSC. Solid State Ionics 177:1091–1097

37. Pandey GP, Agrawal RC, Hashmi SA (2009) Magnesium ion-conducting gel polymer electrolytes dispersed with nanosized magnesium oxide. J Power Sources 190:563–572

38. Kumar GG, Munichandraiah N (2002) Poly (methylmethacrylate)—magnesium triflate gel polymer electrolyte for solid state magnesium battery application. Electrochim Acta 47:1013–1022

39. Zhou DY, Wang GZ, Li WS, Li GL, Tan CL, Rao MM, Liao YH (2008) Preparation and performances of porous polyacrylonitrile-methyl methacrylate membrane for lithium-ion batteries. J Power Sources 184:477–480

40. Lee K-H, Lee Y-G, Park J-K, Seung D-Y (2000) Effect of silica on the electrochemical characteristics of the plasticized polymer electrolytes based on the P(AN-co-MMA) copolymer. Solid State Ionics 133:257–263

41. Kumar D, Hashmi S a. (2010) Ion transport and ion-filler-polymer interaction in poly(methyl methacrylate)-based, sodium ion conducting, gel polymer electrolytes dispersed with silica nanoparticles. J Power Sources 195:5101–5108

42. Pandey GP, Agrawal RC, Hashmi SA (2011) Performance studies on composite gel polymer electrolytes for rechargeable magnesium battery application. J Phys Chem Solids 72:1408–1413

43. Kuo H-H, Chen W-C, Wen T-C, Gopalan A (2002) A novel composite gel polymer electrolyte for rechargeable lithium batteries. J Power Sources 110:27–33